JREE: Vol. 1, No. 1 (December 2014) 53-63

Research Article

Journal of Renewable Energy and Environment

Journal Homepage: www.jree.ir

Reforming of Biogas over Co- and Cu-Promoted Ni/Al_2O_3-ZrO_2 Nanocatalyst Synthesized via Sequential Impregnation Method

Mahdi Sharifi[a,b], Mohammad Haghighi[*a,b], Farhad Rahmani [a,b], Nader Rahemi [a,b]

[a] *Department of Chemical Engineering, Sahand University of Technology, Tabriz, Iran*
[b] *Department of Reactor and Catalysis Research Center (RCRC), Sahand University of Technology, Tabriz, Iran*

Article History
Received: 2 Nov. 2013 Received in revised form: 17 April 2014 Accepted: 15 June 2014 Available online: 17 Sep. 2014

A B S T R A C T

Utilization of active and stable nanocatalyst could have enormous advantages in industrial application of biogas reforming. In order to achieve this goal, the effects of Cu and Co as promoters were investigated over physical-chemical properties of Ni/Al_2O_3-ZrO_2 nanocatalyst in reforming of biogas. The sequential impregnation was used for preparation of nanocatalysts. The nanocatalysts were characterized using XRD, FESEM, BET and FTIR analysis. The XRD patterns displayed that the active phases promoters could be effective on nanoparticles dispersion. The FESEM images showed that uniformity of particle size had improved for bimetallic nanocatalysts in comparison with Ni/Al_2O_3-ZrO_2 nanocatalyst. However, the specific surface areas showed no significant change in BET analysis. Higher content of –OH structural groups on surface of Ni-Co/Al_2O_3-ZrO_2 nanocatalyst were proved by FTIR characterization. The performances of nanocatalysts were assessed at atmospheric pressure, feed gas ratio of CO_2/CH_4= 1, GHSV=24 l/g.h and temperature ranges from 550-850°C. The results revealed that Ni-Co/Al_2O_3-ZrO_2 nanocatalysts had the best activity. Because of optimized operating conditions and application of ZrO_2 as a promoter, the activities of all nanocatalysts remained stable at 850°C for 24 h.

Keywords: Dry Reforming, Biogas, Syngas, Promoted Ni/Al_2O_3-ZrO_2, Impregnation.

1. Introduction

Concern about the high dependence of our economies on crude oil has generated increasing interest in the use of alternative fuel sources. Biogas, which is produced by anaerobic digestion of biomass, is one of the most attractive renewable energy sources available [1-3]. The main composition of biogas usually lies within the ranges of 50-70% CH_4, 25-50 % CO_2;

therefore it could be a cheap and available feedstock for Dry Reforming of Methane process (DRM), or in other words, Bio Gas Reforming (BGR) [1-5]. The disadvantages of this process are the carbon deposition and sintering of active phases due to the high operational temperatures [2-7]. Past studies have shown that Ni/Al_2O_3 catalyst had higher activity and more economical advantages compared to other catalysts at BGR process, but the activity of this catalyst has not been stable. Carbon deposition and active phase sintering were the main reasons for this phenomenon [5, 6, 8-11].

* Corresponding author. *Email: haghighi@sut.ac.ir*

Assessments revealed that methane conversion has decreased about 20 to 25% in less than 10 hours [6, 9, 12]. Utilization of promoters is a suitable and effective way for improvement of catalysts activity [6, 13-16]. Zhang et. al used Mn, Cu, Co, Fe as Ni promoters over $AlMgO_x$ for DRM process. Their results have shown that the stability increases by addition of Co and Cu [4]. Xu et. al have asserted that 3wt% cobalt is the best composition for Ni-Co bimetallic catalyst [1]. It has been proved that the Ni-Co catalyst exhibits active phases with small size and excellent dispersion [5, 8, 13, 17-19]. The CO_2 activation was enhanced over the small metal particles, which is a dam against the coke deposition [20-24]. According to Le Chatelier's principle, the reverse Boudouard reaction (Eq.(1)) will proceed when the CO_2 adsorption increases [18].

$$CO_2 + C\text{-}M \rightarrow 2CO + M \quad (1)$$

The catalyst stability has improved by Ni-Co alloy production due to increasing the active metal oxidation resistance [1, 19]. On the other hand, the addition of Cu as a promoter to Ni/Al_2O_3, increases methane decomposition. Also, it can modify the Ni ensemble environment by the Cu–Ni alloy formation, suppressing the coke formation. Reduction improvement [16, 25] and low content of coke deposition are some benefits of Ni-Cu bimetallic catalyst application for methane decomposition reaction [3, 26]. The stability enhanced by increasing of reaction temperature, while decreased at high temperatures due to the sintering of active phase and coke deposition [16, 26]. Lee and et al. [27] showed that the carbon deposition on $Cu(1\%wt)Ni/Al_2O_3$ catalyst was minimized during CO_2 reforming of methane and it was enhanced on $Cu(x\ wt.\%)\ Ni/Al_2O_3$ ($x \geq 5$) catalysts in comparison with the Ni/Al_2O_3 catalyst [27]. Thus, cobalt and copper were chosen as active promoter components to meet the discussed properties and evaluate their effects, comparatively. Also, in another study of our groups, the performance of $Ni\text{-}Co/Al_2O_3$ and $Ni\text{-}Cu/Al_2O_3$ catalyst were evaluated in dry reforming of methane [21]. These catalysts were synthesized via sol-gel and impregnation methods without any promoters. The evaluation has shown that $Ni\text{-}Co/Al_2O_3$ catalyst synthesized via sol-gel method had the best properties and performance.

Different materials were applied as support promoter, but ZrO_2 had particular effects on physic-chemical properties of Ni/Al_2O_3 catalyst [6, 12, 28-32]. ZrO_2 acts as a barrier against entrance of active phase to alumina structure and spinel production. The spinels components decrease the activity of active phases due to the fact that the spinels reduction is very hard [6, 33]. ZrO_2 is known as an acid-base bi-functional catalyst. According to reactant species in the process environment, it could be an acid or base catalyst [34]. CO_2 is the acid gas, so ZrO_2 acts as a base catalyst in BGR process. In other words, addition of ZrO_2 decreases the coke deposition due to more CO_2 adsorption to remove coke deposition through reverse Boudouard reaction [6, 12, 28, 35]. 10%wt of Ni and ZrO_2 were the optimized composition for $Ni/Al_2O_3\text{-}ZrO_2$ catalyst in DRM process [6, 35, 36].

Utilizing a simple and effective method provides economical advantages and it can be effective in industrial applications. The evaluations have indicated that imperegnation method is a simple and economical method for catalysts preparation [6, 35].

Therefore, it seems that by using the best composition of suitable promoters and implementing proper preparation method, $Ni/Al_2O_3\text{-}ZrO_2$ nanocatalyst could be a promising nanocatalyst for BGR process. To this aim, the effect of Co and Cu addition as active phase promoters were assessed on $Ni/Al_2O_3\text{-}ZrO_2$ nanocatalyst performance. The synthesized nanocatalysts were characterized by XRD, FESEM, BET and FTIR analysis. Biogas was simulated with CH_4 and carbon dioxide in a molar ratio of 1 and without dilute gas. Nanocatalysts performance were evaluated as function of reaction temperature from 550 to 850°C in atmospheric pressure and 40ml/min flow rate (GHSV= 24 l/g.h). There are some differences between this research and our last study [21] such as

synthesis method and utilization of support promoters.

2. Materials and Methods

2.1. Materials

The unprompted and Co and Cu-promoted 3%wt of Ni (10%wt)/Al_2O_3- ZrO_2 (10%wt) nanocatalysts were prepared by a sequential impregnation method. The $Ni(NO_3)_2$. $6H_2O$ (supplied by Merck Co.) and $Zr(NO_3)_2$.$5H_2O$ (supplied by Aldrich) were utilized as active metal and support promoter precursors, respectively. Al_2O_3 powder (Merck Co.) was used as the support. For promotion of active phase, $Co(NO_3)_2.6H_2O$ and $Cu(NO_3)_2.3H_2O$ (Merck Co.) were impregnated with Ni precursor onto Al_2O_3-ZrO_2.

2.2. Nanocatalyst Preparation and Procedure

Schematic flowchart for the preparation steps of the nanocatalysts synthesized by impregnation method is shown in Fig.1. At first, appropriate amounts of zirconia precursor and γ-alumina powder were dissolved in de-ionized water and mixed. After drying and calcination, the support of Al_2O_3-ZrO_2 was prepared. For addition of active phases in this stage, nickel nitrate hexahydrate and cobalt or cooper nitrate hexahydrate were dissolved in de-ionized water and prepared support was added to the solution. Mixing, drying and calcination were similar to the prior stage.

2.3. Nanocatalyst Characterization Thechniqe

The XRD analysis was used for evaluation of phase structures of the nanocatalysts (Bruker model D8 advance, Germany). X-Ray diffractometer with Cu Kα (λ = 1.54178 ˚A) with scanning rate and scanning range 0.03◦/s (2θ) 20–90°, respectively. The morphology and particle size of the nanostructure nanocatalysts assessed by Field Emission Scanning Electron Microscopy (FESEM) analyser (HITACHI S-4160 or VEGA TESCAN). The specific BET surface area was determined by N2 adsorption–desorption measurements at liquid-nitrogen temperature (Quanta chrome chembet-3000). Surface functional groups were studied by Fourier

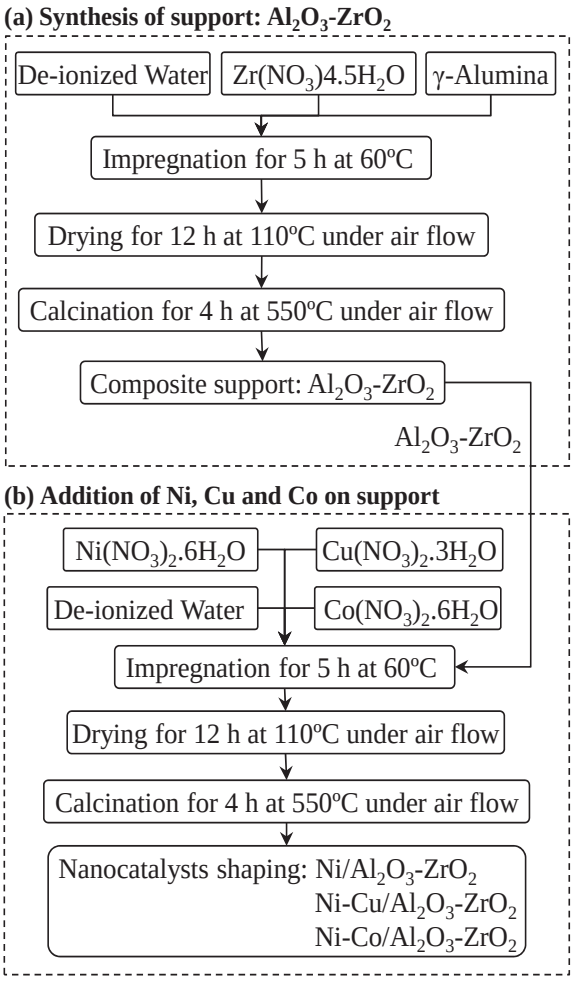

Fig. 1. Preparation steps of Ni/Al_2O_3-ZrO_2 , Ni-Cu/Al_2O_3-ZrO_2 and Ni-Co/Al_2O_3-ZrO_2 nanocatalysts via sequential impregnation method.

Transform Infrared Spectroscopy (FTIR, MATTSON 1000). The wave number's range at this characterization was 400–4000 cm^{-1}.

2.4. Experimental Setup for Catalytic Performance Test

The schematic of the experimental setup for activity testing of the nanocatalysts is illustrated in Fig. 2. The CO_2 reforming of methane was carried out at atmospheric pressure in an 8 mm i.d. U-shape quartz tube packed bed reactor loaded with 0.1g of the nanocatalyst. First, the nanocatalysts reduction were done at 700°C under hydrogen stream with a flow rate of 30 ml/min for 3 h. CH_4 and CO_2 gases were fed into the reactor controlled by mass flow

controllers (MFC, Beijing Seven star Electronics Co., Ltd.). Evaluation of catalytic performance of prepared catalysts was performed over the temperature range of 550–850°C. The total flow rate was set at 40 ml/min during activity tests. For stability tests, gas mixture of 50% CH_4/ 50% CO_2 is introduced through the catalytic bed at 850 °C and total flow rate of 40 mL/min during 24 h. The reactants and products were analysed using an on-line gas chromatograph (GC Chrom, Teif Gostar Faraz, Iran) equipped with Agilent molecular sieve and Plot-U columns as well as TCD and FID detectors. In this work, feed conversion (CH_4 and CO_2) and yield of products (CO and H_2) were calculated from the following formulas:

$$X_{CH_4}\% = \frac{C_{CH_{4in}} - C_{CH_{4out}}}{C_{CH_{4in}}} \times 100 \quad (2)$$

$$X_{CO_2}\% = \frac{C_{CO_{2in}} - C_{CO_{2out}}}{C_{CO_{2in}}} \times 100 \quad (3)$$

$$Y_{H_2}\% = \frac{C_{H_{2out}}}{2C_{CH_{4in}}} \times 100 \quad (4)$$

$$Y_{CO}\% = \frac{C_{CO_{out}}}{C_{CH_{4in}} + C_{CO_{2in}}} \times 100 \quad (5)$$

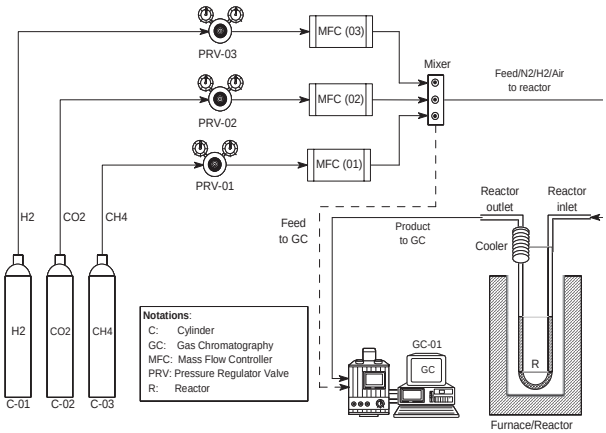

Fig. 2. Experimental setup for evaluation of Ni/Al_2O_3-ZrO_2, Ni-Cu/Al_2O_3-ZrO_2 and Ni-Co/Al_2O_3-ZrO_2 nanocatalysts toward reforming of biogas.

3. Results and Discussions

3.1. Nanocatalyst Characterizations

3.1.1 XRD Analysis

Figure 3 shows the X-ray diffraction spectra of the pure γ-Al_2O_3, Ni/Al_2O_3-ZrO_2, Ni-Cu/Al_2O_3-ZrO_2 and Ni-Co/Al_2O_3-ZrO_2 nanocatalysts calcined at 550°C. In pattern (a), the peaks of γ-Al_2O_3 were observed at 2θ =37.4°, 39.7°, 42.8°, 45.8° and 67.3° (JCPDS: 00-004-0880). It can be identified from the figure that the patterns confirm formation of γ-Al_2O_3 phase and also NiO phase at 2θ =37.3°, 43.4°, 63.0°, 75.6° and 79.6° (JCPDS: 01-073-1519). The average crystallite size of γ-Al_2O_3 and NiO phases for pattern (b) are 15.9 nm and 9.5 nm, respectively which were derived by Scherrer equation. The intensity of nickel peaks somewhat have declined after Cu and Co addition. The improvement of dispersion could be a reason for this behaviour. Considering the fact that percentage of zirconia was low, there were just two weak peaks for t-ZrO_2 phases at 2θ =30.2° and 50.3° (JCPDS: 01-080-0784) and no more peaks were observed due to overlapping with other phases.

The impregnation method is not capable of preventing spinel production due to the low distribution and weak dispersion of ZrO_2 among Ni and Al_2O_3 structures. Therefore, a clear XRD peak of $NiAl_2O_4$ spinel was observed at 2θ =19.1° (JCPDS: 00-010-0339) for all catalysts. The other peaks of $NiAl_2O_4$ spinel had overlaps with γ-Al_2O_3, NiO and ZrO_2 peaks. For example, the peaks of $NiAl_2O_4$ at 2θ of 31.4º and 37° are severely covered by the peaks of γ-Al_2O_3, NiO and ZrO_2. Also, the interaction between ZrO_2 and Al_2O_3 could produce Al_2O_3-ZrO_2 composite layer which is an amorphous phase or a crystalline phase with crystallite sizes smaller than the detection limit of XRD. The alumina peaks have shifted to lower angels in samples (b)-(d) relative to pure Al_2O_3 due to the production of spinel and Al_2O_3-ZrO_2 composite. Also, comparison of the patterns shows that Al_2O_3 peaks intensity has decreased; it seems that improvement of nanoparticles dispersion could be a reason for this phenomena. Co and Cu compositions are very low (3%wt) in samples (c) and (d); therefore there were no peaks in their XRD pattern. The comparison between these results and our last study shows that sol-gel method was more effective than addition of

support promoter. The amount of spinel productions in synthesized catalyst via sol-gel method (Ni-Co/Al_2O_3) was lower than Ni-Co/Al_2O_3-ZrO_2 catalyst.

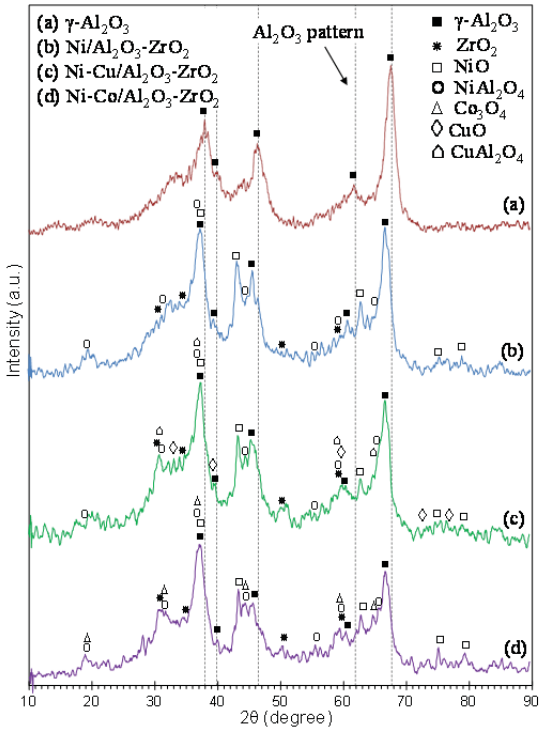

Fig. 3. XRD patterns of the support: (a) γ-Al_2O_3 and synthesized nanocatalysts: b) Ni/Al_2O_3-ZrO_2, (c) Ni-Cu/Al_2O_3-ZrO_2 and (d) Ni-Co/Al_2O_3-ZrO_2.

3.1.2 FESEM Analysis

Figure 4 displays the FESEM images of pure γ-Al_2O_3 (a), Ni/Al_2O_3-ZrO_2 (b), Ni-Cu/Al_2O_3-ZrO_2 (c) and Ni-Co/Al_2O_3-ZrO_2 (d) catalysts. As can be seen in Fig. 4 (b) after addition of Ni and ZrO_2 to pure γ-Al_2O_3 by impregnation method, the particle size has increased as far as they were out of nanometer scale. The control of particle size is weak in impregnation method; therefore, distribution of particles in pure alumina was more uniform than Ni/Al_2O_3-ZrO_2 nanocatalyst. The uniformity of nanoparticles has improved by Cu and Co addition. It seems that the surface roughness has decreased by addition of promoters, as can be seen in FESEM analysis; therefore, catalysts surface area could be changed. The FESEM results of Ni-Co/Al_2O_3 (Sol-gel) in Sajjadi's studies [21] showed uniformity of particles size were very high and there were no sintering of particles. But, in this study, there were some agglomeration for particles in Ni-Co/Al_2O_3-ZrO_2 catalyst synthesized via impregnation method. This phenomenon revealed that sol-gel is more effective than impregnation method.

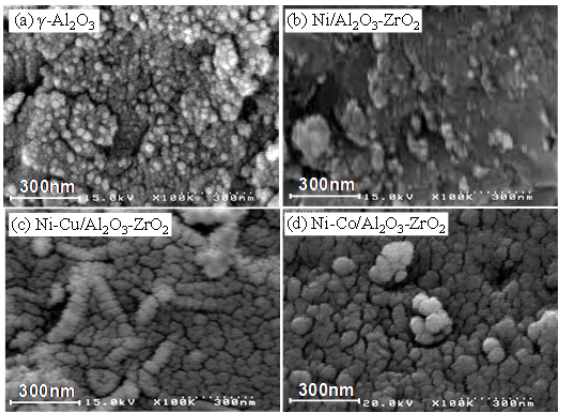

Fig. 4. FESEM images of support: (a) γ-Al_2O_3 and synthesized nanocatalysts: b) Ni/Al_2O_3-ZrO_2, (c) Ni-Cu/Al_2O_3-ZrO_2 and (d) Ni-Co/Al_2O_3-ZrO_2.

3.1.3 BET Analysis

Figure 5 illustrates the total specific surface area, S_{BET}, of calcined samples by a bar chart. By addition of active metals and ZrO_2 to Al_2O_3 the surface area has decreased. In these cases, loading of Zr and active metals would lead to the blockage of alumina pores resulting in surface area reduction for nanocatalysts. Also, difference between surface areas of nanocatalysts was very low due to the low content of Cu and Co in Ni-Cu/Al_2O_3-ZrO_2 and Ni-Co/Al_2O_3-ZrO_2 nanocatalysts. Ni-Co/Al_2O_3-ZrO_2 nanocatalyst had the lowest surface area (79 m^2/g). The higher particles agglomerations of this nanocatalyst compared to other samples are the reason for this phenomenon observed in FESEM analysis. In our recent study [21] Ni-Co/Al_2O_3 catalyst was synthesized via sol-gel method and the BET analysis showed specific surface area of this catalyst to be 257 m^2/g. But, after addition of ZrO_2 by impregnation method to Al_2O_3 and Ni-Co, the BET surface area decreased (79 m^2/g). This result shows that alumina pores could be blocked by ZrO_2. Furthermore, the smaller and more uniform particle sizes were

produced via sol-gel method in comparison with impregnation method. The FESEM results confirmed these observations.

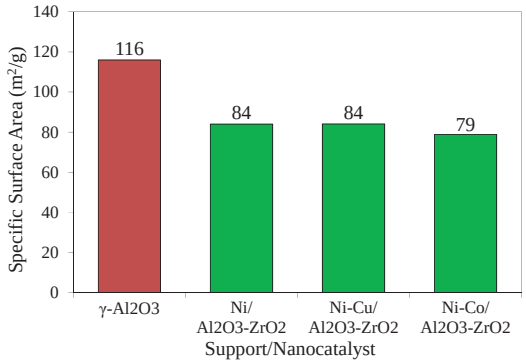

Fig. 5. BET specific surface area of support and synthesized nanocatalysts.

3.1.4 FTIR Analysis

Figure 6 presents the FTIR spectra of the synthesized samples. There are some tiny bendings before 500 cm^{-1} which are attributed to different vibration of M–O (metal oxide) bonds (Al–O, Zr–O, Ni–O, Cu–O and Co–O) [37-40]. The low-energy region of the synthesized nanocatalysts spectra between 500-1000 cm^{-1} are attributed to the deformation vibration of the link Zr–O–Al [39]. The amorphous state is responsible for the low level definition of this band in the region which confirms the obtained results from XRD characterization about the high metal dispersion and the formation of Al_2O_3-ZrO_2 composite layer. At region 1500-2000 cm^{-1} the stretching vibration of adsorbed water (deformation vibration) have seen and 3000-4000 cm^{-1}(symmetric and asymmetric vibration) wave number are observed for all samples [37, 38, 40, 41]. The bands of Al–OH and Zr–OH (hydroxyl groups) could be seen at 1000-1500 and 3000-4000 cm^{-1} wave numbers which the Ni-Co/Al_2O_3-ZrO_2 nanocatalyst had more powerful vibration than other samples at this region. This phenomenon demonstrates that Ni-Co/Al_2O_3-ZrO_2 nanocatalyst has high potential for CO_2 adsorption and it is confirmed by the stronger stretching vibration of adsorbed CO_2 in atmosphere (2370 cm^{-1} wave number) on the surface of Ni-Co/Al_2O_3-ZrO_2 compared to other samples. It seems that the presence of cobalt was effective in CO_2 adsorption which is confirmed by Li et. al. [13]. Higher content of –OH structural groups on the surface promotes the basicity of the catalyst. Therefore, it leads to enhance the adsorption of acidic CO_2. Consequently, activity and life time of the catalyst would be modified due to the enhancement of DRM reaction and reverse Boudouard reaction.

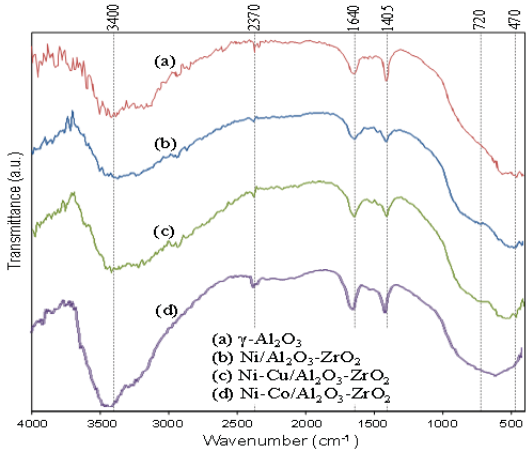

Fig. 6. FTIR spectrum of support: (a) γ-Al_2O_3 and synthesized nanocatalysts: (b) Ni/Al_2O_3-ZrO_2, (c) Ni-Cu/Al_2O_3-ZrO_2 and (d) Ni-Co/Al_2O_3-ZrO_2.

3.2 Catalytic Performance Study toward CO_2 Reforming of Methane

3.2.1 Effect of Nanocatalyst Type on Feed Conversion

Effect of temperature on CH_4 and CO_2 conversions is shown in Figure 7. The experiments for activity tests were carried out at constant molar feed ratio (CH_4/CO_2 = 1), gas hourly space velocity (GHSV = 24 l/g.h) and total pressure of 1 atmosphere. Thermodynamic equilibrium becomes favorable at higher temperatures due to the endothermic property of biogas reforming reaction. Therefore, as can be seen, the feed conversion rises slowly with increasing the reaction temperature. Ni-Co/Al_2O_3-ZrO_2 nanocatalyst has the best activity at 850°C (X_{CH4}= 91.05%, X_{CO2}= 93.7%). Some side reactions (reverse water gas shift reaction and reverse Boudouard reaction) occur with the main reaction simultaneously. They create the inequality of reactants conversion and change in the desired stoichiometry molar

ratio. At higher temperatures, the effect of side reactions reduces as a result of dramatic increase of the equilibrium constant [4, 18, 42, 43]. Therefore, there is no significant difference between both reactants conversion at high temperatures. Besides, thermodynamic stability of methane in low temperature and easy decomposition of C–H bounds at high temperature could be another reasons. Regarding the fact that copper aggregates at high temperatures [16, 26, 27], Ni-Cu alloy has maximum potential for active phase sintering. It seems that this is a reason for lower activity of Ni-Cu/Al_2O_3-ZrO_2 than other nanocatalysts. Li et al. have proved that Ni-Co had higher ability for CO_2 adsorption than mono metallic catalysts (Ni and Co) [13]. Besides, some new base sites could be added to raise CO_2 adsorption. That is a result of utilizing Co as promoter. It can be found that Co addition reinforces activity of Ni for CH_4 decomposition and CO_2 dissociation.

3.2.2 Effect of Nanocatalyst Type on Product Yield

Evaluation of products yield is displayed in Fig. 8. The Ni-Co/Al_2O_3-ZrO_2 nanocatalyst has the best results at 850°C (Y_{H2}= 92.14%, Y_{CO}= 93.91%). Also, the activity of Ni-Cu/Al_2O_3-ZrO_2 nanocatalyst was weaker than others, probably due to the sintering of active phases. The general trend of changes for products yield is similar to the feed conversion data. All reasons explained in pervious section are expressible for observations in the figure.

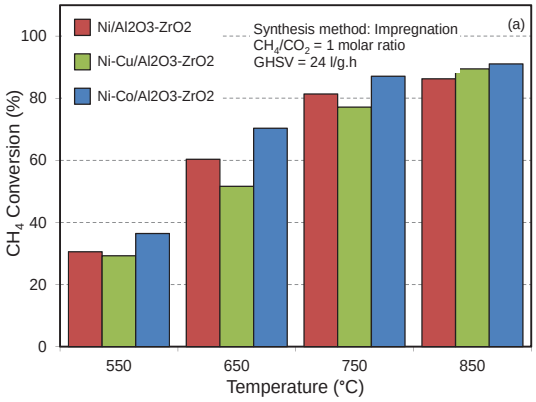

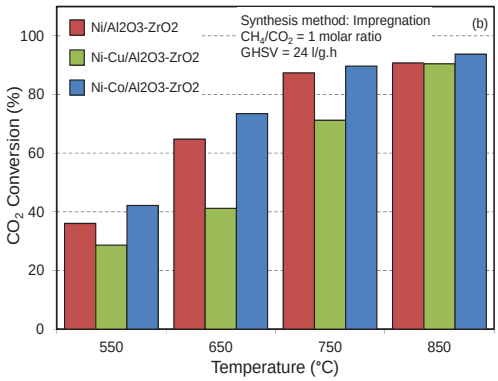

Fig. 7. Effect of temperature on feed conversion over Ni/Al_2O_3-ZrO_2, Ni-Cu/Al_2O_3-ZrO_2 and Ni-Co/Al_2O_3-ZrO_2 nanocatalysts: (a) CH_4 conversion and (b) CO_2 conversion.

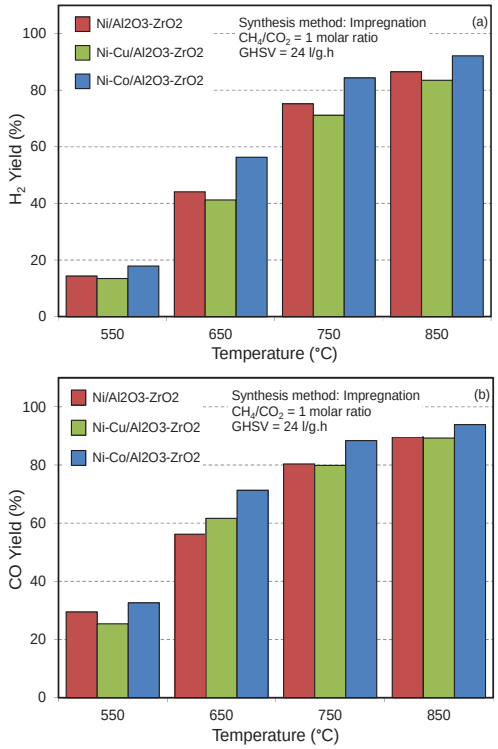

Fig. 8. Effect of temperature on products yield over Ni/Al_2O_3-ZrO_2, Ni-Cu/Al_2O_3-ZrO_2 and Ni-Co/Al_2O_3-ZrO_2 nanocatalysts: (a) H_2 yield and (b) CO yield.

3.2.3 Effect of Nanocatalyst Type on H2/CO Ratio in Product

The effect of temperature on H_2/CO molar ratio over Ni/Al_2O_3-ZrO_2, Ni-Cu/Al_2O_3-ZrO_2 and Ni-Co/Al_2O_3-ZrO_2 nanocatalysts is shown in Fig. 9. The best ratio (0.972) was obtained at 850°C for Ni-Co/Al_2O_3-ZrO_2 nanocatalyst. By rising temperature, syngas

ratio has enhanced. H_2 consumption in reverse water gas shift reaction and CO production in reverse Boudouard reaction change syngas molar ratio; therefore, H_2/CO molar ratio is not equal to stoichiometry ratio. Thermodynamic assessment at the reported studies [4, 42, 43] has revealed that the effect of side reactions decrease at high temperature and also, the equilibrium constant of main reaction increases due to the endothermic property. Therefore, the product yield and syngas molar ratio have improved.

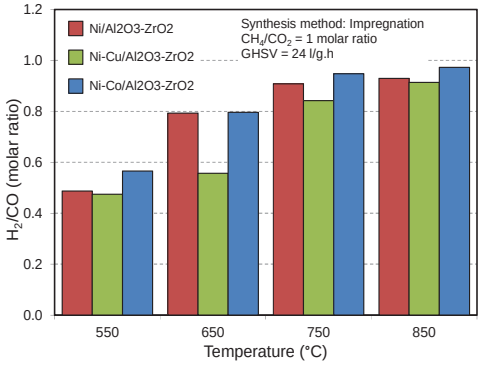

Fig. 9. Effect of temperature on H_2/CO molar ratio in product over Ni/Al_2O_3-ZrO_2, Ni-Cu/Al_2O_3-ZrO_2 and Ni-Co/Al_2O_3-ZrO_2 nanocatalysts.

3.2.4 Time on Stream Performance

In industrial scale operations, in order to improve nanocatalyst activity and selectivity it is quite typical to increase the operation temperature, but it may affect the stability or durability of a nanocatalyst especially for DRM process in future. Therefore, further studies on the stability of synthesized nanocatalysts were performed. In Fig. 10, the products yield and H_2/CO ratio during 24 h, constant temperature (850°C), feed ratio (CH_4/CO_2 = 1) and GHSV (24 L/g.h) are plotted. No activity reduction is observed over the synthesized nanocatalysts. According to literature, major reason for impregnated Ni/Al_2O_3 nanocatalysts deactivation is coke formation [6, 11, 35]. Carbon formation via methane decomposition is more probable in structure defects for impregnated Ni/Al_2O_3 catalysts [44, 45]. As can be seen, activity of all nanocatalysts remains stable for 24 h. Zirconia in this process acts as a base active phase which can enhance CO_2 activation. On the other hand, this metal oxide can play the role of a barrier against active phase sintering. As the FTIR results showed, there were –OH functional groups on nanocatalysts surface. The –OH functional groups at these nanocatalysts are CO_2 adsorption agent. Accordingly, ZrO_2 reflects suitable effect on stability of nanocatalysts. Moreover, application of proper operating conditions for biogas reforming process was effective on good stability of nanocatalysts.

Finally, the comparison between activity of Ni-Co/Al_2O_3-ZrO_2 catalyst (in this study) and Ni-Co/Al_2O_3 catalyst (in our last study) [21] is essential. The results revealed that Ni-Co/Al_2O_3 catalyst which is synthesized via sol-gel method (as denoted NCo/Al-SG) had the higher activity than Ni-Co/Al_2O_3-ZrO_2 catalyst is synthesized via impregnation method (as denoted NCo/AlZr-I) at all temperatures. As mentioned in the past sections, NCo/Al-SG had higher surface area and smaller particle size compared to NCo/AlZr-I catalyst. These properties confirm the observations for activity of catalysts. The activity of all catalysts was stable during 1440 min in both researches.

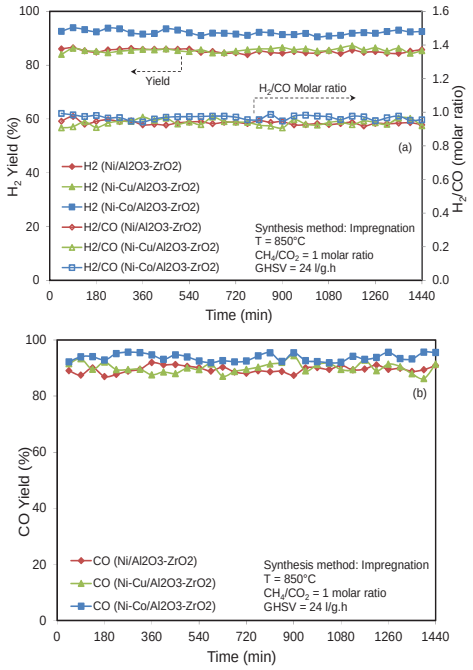

Fig. 10. Time on stream performance of synthesized nanocatalysts: (a) H_2 yield and H_2/CO molar ratio and (b) CO yield.

4. Conclusions

The results of this study displayed that correct choice and application of promoters can be effective on nanocatalyst physic-chemical properties in Bio Gas Reforming (BGR) process. The evaluation revealed that the Co addition to Ni/Al_2O_3-ZrO_2 nanocatalyst was more effective in activity than the Cu utilization. The XRD results showed that spinel phase are produced and ZrO_2 addition by impregnation method has not prevented spinel production. The FESEM images revealed that Co and Cu have improved uniformity of particles size but the BET surface area of nanocatalysts has remained relatively constant. The surface area of γ-Al_2O_3 decreased after loading of Zr and active metals over alumina and led to the blockage of alumina pores. The FTIR analysis displayed that $Ni\text{-}Co/Al_2O_3$-ZrO_2 nanocatalyst had the greater potential for CO_2 adsorption than other samples. The best activity was gained for $Ni\text{-}Co/Al_2O_3$-ZrO_2 nanocatalyst while $Ni\text{-}Cu/Al_2O_3$-ZrO_2 nanocatalyst had lower activity, probably due to the sintering of Cu active phase. Also, proper operating conditions and application of promoter, in particular ZrO_2, led to stability of nanocatalysts during 24 h and 850°C in bio gas reforming. It seems that the stability of nanocatalysts during longer time and application of modern synthesized methods can be subjects for future researches.

5. Acknowledgements

The authors gratefully acknowledge Sahand University of Technology for the financial support of the research as well as Iran Nanotechnology Initiative Council for complementary financial support.

6. References

1. Xu J., Zhou W., Li Z., Wang J., Ma J Biogas reforming for hydrogen production over nickel and cobalt bimetallic catalysts. Int J Hydrogen Energy, 2009, 34(16), 6646-6654.
2. Avraam D.G., Halkides T.I., Liguras D.K., Bereketidou O.A., Goula M.A. An experimental and theoretical approach for the biogas steam reforming reaction. Int J Hydrogen E, 2010, 35(18), 9818-9827.
3. Bonura G., Cannilla C., Frusteri F. Ceria-gadolinia supported NiCu catalyst: A suitable system for dry reforming of biogas to feed a solid oxide fuel cell (SOFC). Appl Catal, B, 2012, 121-122, 135-147.
4. Zhang J., Wang H., Dalai A. Development of stable bimetallic catalysts for carbon dioxide reforming of methane J Catal, 2007, 249(2), 300-310.
5. San Jose-Alonso D., Illan-Gomez M.J., Roman-Martinez M.C. Low metal content Co and Ni alumina supported catalysts for the CO_2 reforming of methane. Int J Hydrogen E, 2013, 38(5), 2230-2239.
6. Therdthianwong S., Siangchin C., Therdthianwong A. Improvement of coke resistance of Ni/Al_2O_3 catalyst in CH_4/CO_2 reforming by ZrO_2 addition. Fuel Process Technol, 2008, 89(2), 160-168.
7. Ruckenstein E., Hu Y.H. Carbon dioxide reforming of methane over nickel alkaline earth metal oxide catalysts. Appl Catal, A, 1995, 133, 149-161.
8. San-Jose-Alonso D., Juan-Juan J., Illan-Gomez M.J., Roman-Martinez M.C. Ni, Co and bimetallic Ni-Co catalysts for the dry reforming of methane. Appl Catal, A, 2009, 371(1-2), 54-59.
9. Pompeo F., Nichio N., Ferretti O., Resasco D. Study of Ni catalysts on different supports to obtain synthesis gas. Int J Hydrogen E, 2005, 30(13-14), 1399-1405.
10. Hao Z., Zhu Q., Jiang Z., Hou B., Li H. Characterization of aerogel Ni/Al_2O_3 catalysts and investigation on their stability for CH_4-CO_2 reforming in a fluidized bed Fuel Process Tech, 2009, 90(1), 113-121.
11. Halliche D., Bouarab R., Cherifi O., Bettahar MM. Carbon dioxide reforming of methane on modified Ni/α-Al_2O_3 catalysts Catal Today, 1996, 29(1-4), 373-377.
12. Pompeo F., Nichio N.N., Souza M.M.V.M., Cesar D.V., Ferretti O.A., Schmal M. Study of Ni and Pt catalysts supported on α-Al_2O_3 and ZrO_2 applied in methane reforming with CO_2. Appl Catal, A, 2007, 316(2), 175-183.
13. Li X., Ai J., Li W., Li D. Ni-Co bimetallic catalyst for CH_4 reforming with CO_2. F. Chem Eng China, 2010, 4(4), 476-480.

14. Nagaraja B.M., Bulushev D.A., Beloshapkin S., Ross J.R.H. The effect of potassium on the activity and stability of Ni-MgO-ZrO_2 catalysts for the dry reforming of methane to give synthesis gas CatalToday, 2011, 178(1), 132-136.
15. Foo S.Y., Cheng C.K., Nguyen T.-H., Adesina A.A. Kinetic study of methane CO_2 reforming on Co-Ni/Al_2O_3 and Ce-Co-Ni/Al_2O_3 catalysts Catal Today, 2011, 164(1), 221-226.
16. Li D., Chen J., Li Y. Evidence of composition deviation of metal particles of a Ni-Cu/Al_2O_3 catalyst during methane decomposition to CO_x-free hydrogen. Int J Hydrogen E, 2009, 34(1), 299-307.
17. Roberts C.B., Elbashir N.O. An overview to 'Advances in C1 chemistry in the year 2002'. Fuel Process Tech, 2003, 83, 1-9.
18. Zhang J., Wang H., Dalai A.K. Effects of metal content on activity and stability of Ni-Co bimetallic catalysts for CO_2 reforming of CH_4. Appl Catal, A, 2008, 339(2), 121-129.
19. Djinovic P., Crnivec O, Gasan I., Erjavec B., Pintar A. Influence of active metal loading and oxygen mobility on coke-free dry reforming of Ni-Co bimetallic catalysts. Appl Catal, B, 2012, 125, 259-270.
20. Vafaeian Y., Haghighi M., Aghamohammadi S. Ultrasound Assisted Dispersion of Different Amount of Ni over ZSM-5 Used as Nanostructured Catalyst for Hydrogen Production via CO2 Reforming of Methane E Convers. Manage, 2013, 76, 1093-1103.
21. Sajjadi S.M., Haghighi M., Alizadeh Eslami A., Rahmani F. Hydrogen Production via CO2-Reforming of Methane over Cu and Co Doped Ni/Al2O3 Nanocatalyst: Impregnation vs. Sol-Gel Method and Effect of Process Conditions and Promoter. J Sol-Gel Sci Tech, 2013, 67(3), 601-617.
22. Rahemi N., Haghighi M., Babaluo A.A., Fallah Jafari M., Khorram S. Conversion of CH4/CO2 to Syngas over Ni-Co/Al2O3-ZrO2 Nanocatalyst Synthesized via Plasma Assisted Co-impregnation Method: Surface Properties and Catalytic Performance. J Appl Phys, 2013, 114(9), 0943011-09430110.
23. Rahemi N., Haghighi M., Babaluo A.A., Fallah Jafari M., Estifaee P. CO2 Reforming of CH4 Over CeO2-Doped Ni/Al2O3 Nano catalyst Treated by Non-Thermal Plasma. J Nanosci. Nanotech, 2013, 13(7), 4896-4908.
24. Aghamohammadi S., Haghighi M., Karimipour S. A Comparative Synthesis and Physicochemical Characterizations of Ni/Al2O3-MgO Nanocatalyst via Sequential Impregnation and Sol-Gel Methods Used for CO2 Reforming of Methane J Nanosci. Nanotech, 2013, 13(7), 4872-4882.
25. Lopez P., Mondragon-Galicia G., Espinosa-Pesqueira M.E., Mendoza-Anaya D., Fernandez ME., Gomez-Cortes A., Bonifacio J., Martínez-Barrera G., Perez-Hernandez R. Hydrogen production from oxidative steam reforming of methanol: Effect of the Cu and Ni impregnation on ZrO_2 and their molecular simulation studies. Int J Hydrogen E, 2012, 37(11), 9018-9027.
26. Reshetenko T.V., Avdeeva L.B., Ismagilov Z.R., Chuvilin A.L., Ushakov V.A. Carbon capacious Ni-Cu-Al_2O_3 catalysts for high-temperature methane decomposition. Appl Catal, A, 2003, 247(1), 51-63.
27. Lee J-H., Lee E.G., Joo O.-S., Jung K.-D. Stabilization of Ni/Al_2O_3 catalyst by Cu addition for CO_2 reforming of methane. Appl Catal, A, 2004, 269, 1-6.
28. Rahemi N., Haghighi M., Babaluo AA., Jafari MF, Estifaee P. Synthesis and physicochemical characterizations of Ni/Al_2O_3-ZrO_2 nanocatalyst prepared via impregnation method and treated with non-thermal plasma for CO_2 reforming of CH_4. J Ind Eng Chem, 2013, 19(5), 1566-1576.
29. Qian L., Yan Z.F. Study on the Reaction Mechanism for Carbon Dioxide Reforming of Methane over supported Ni catalyst. Chin Chem Lett, 2003, 14, 1081-1084.
30. Sosa Vazquez M., Reyes Rojas A., Collins-Martinez V., Lopez Ortiz A. Study of the stabilizing effect of Al_2O_3 and ZrO_2 in mixed metal oxides of Cu for hydrogen production through REDOX cycles Catal Today, 2005, 107-108, 831-837.
31. Han S.J., Bang Y., Seo J.G., Yoo J., Song I.K. Hydrogen production by steam reforming of ethanol over mesoporous Ni-Al_2O_3-ZrO_2 xerogel catalysts: Effect of

Zr/Al molar ratio. Int J Hydrogen E, 2013, 38(3), 1376-1383.
32. Amairia C., Fessi S., Ghorbel A., Rives A. Methane oxidation behaviour over sol-gel derived Pd/Al_2O_3-ZrO_2 materials: Influence of the zirconium precursor J Mol Catal A: Chem, 2010, 332(1-2), 25-31.
33. Seo J.G., Youn M.H., Park S., Chung J.S., Song I.K. Hydrogen production by steam reforming of liquefied natural gas (LNG) over Ni/Al_2O_3-ZrO_2 xerogel catalysts: Effect of calcination temperature of Al_2O_3-ZrO_2 xerogel supports Int J Hydrogen E, 2009, 34(9), 3755-3763.
34. Tanabe K., Yamaguchi T. Acid-base bifunctional catalysis by ZrO_2 and it's mixed oxides Catal Today, 1994(20), 185-198.
35. Therdthianwong S. Synthesis gas production from dry reforming of methane over Ni/Al_2O_3 stabilized by ZrO_2. Int J Hydrogen E, 2008, 33(3), 991-999.
36. Li H., Wang J. Study on CO_2 reforming of methane to syngas over Al_2O_3-ZrO_2 supported Ni catalysts prepared via a direct sol-gel process Chem Eng Sci, 2004, 59(22-23), 4861-4867.
37. Dabbagh H.A., Zamani M. Catalytic conversion of alcohols over alumina-zirconia mixed oxides: Reactivity and selectivity Appl Catal, A, 2011, 404(1-2), 141-148.
38. Abbasi Z., Haghighi M., Fatehifar E., Saedy S. Synthesis and physicochemical characterizations of nanostructured Pt/Al_2O_3-CeO_2 catalysts for total oxidation of VOCs J Hazard Mater, 2011, 186(2-3), 1445-1454.
39. Moran-Pineda M., Castillo S., Lopez T., Gomez R., Cordero B., Novaro O. Synthesis, characterization and catalytic activity in the reduction of NO by CO on alumina-zirconia sol-gel derived mixed oxides Appl Catal, B, 1999, 21(2), 79-88.
40. Ryczkowski J. IR spectroscopy in catalysis Catal Today, 2001, 68(4), 263-381.
41. Sarkar D., Mohapatra D., Ray S., Bhattacharyya S., Adak S., Mitra N. Nanostructured Al_2O_3-ZrO_2 composite synthesized by sol-gel technique: powder processing and microstructure J Mater Sci, 2007, 42(5), 1847-1855.
42. Khoshtinat Nikoo M., Amin N.A.S. Thermodynamic analysis of carbon dioxide reforming of methane in view of solid carbon formation. Fuel Process Tech, 2011, 92(3), 678-691.
43. Haghighi M., Sun Z.-q., Wu J.-h., Bromly J., Wee H.L., Ng E., Wang Y., Zhang D.-k. On the reaction mechanism of CO_2 reforming of methane over a bed of coal char Proceedings of the Combustion Institute, 2007, 31(2), 1983-1990.
44. Kroll V.C.H., Swaan H.M., Mirodatos C. Methane Reforming Reaction with Carbon Dioxide Over Ni/SiO_2 Catalyst: I. Deactivation Studies J Catal, 1996, 161, 409-422.
45. Burghgraef H., Jansen A.P.J., Santen R.A.v. Methane activation and dehydrogenation on nickel and cobalt: a computational study Surf Sci, 1995, 324, 345-356.